J. Fluid Mech. (1971), *vol.* 46, *part* 2, *pp.* 365–383
Printed in Great Britain

Flow and pressure drop in systems of repeatedly branching tubes

By T. J. PEDLEY,† R. C. SCHROTER AND M. F. SUDLOW

Physiological Flow Studies Unit,
Imperial College, London, S.W.7

(Received 14 July 1970)

The airways of the lung form a rapidly diverging system of branched tubes, and any discussion of their mechanics requires an understanding of the effects of the bifurcations on the flow downstream of them. Experiments have been carried out in models containing up to two generations of symmetrical junctions with fixed branching angle and diameter ratio, typical of the human lung. Flow visualization studies and velocity measurements in the daughter tubes of the first junction verified that secondary motions are set up, with peak axial velocities just outside the boundary layer on the inner wall of the junction, and that they decay slowly downstream. Axial velocity profiles were measured downstream of all junctions at a range of Reynolds numbers for which the flow was laminar.

In each case these velocity profiles were used to estimate the viscous dissipation in the daughter tubes, so that the mean pressure drop associated with each junction and its daughter tubes could be inferred. The dependence of the dissipation on the dimensional variables is expected to be the same as in the early part of a simple entrance region, because most of the dissipation will occur in the boundary layers. This is supported by the experimental results, and the ratio Z of the dissipation in a tube downstream of a bifurcation to the dissipation which would exist in the same tube if Poiseuille flow were present is given by

$$Z = (C/4\sqrt{2})\,(Re\,d/L)^{\frac{1}{2}},$$

where L and d are the length and diameter of the tube, Re is the Reynolds number in it, and the constant C (equal to one for simple entry flow) is equal to 1·85 (the average value from our experiments). In general, C is expected to depend on the branching angles and diameter ratios of the junctions used. No experiments were performed in which the flow was turbulent, but it is argued that turbulence will not greatly affect the above results at Reynolds numbers less than and of the order of 10000. Many more experiments are required to consolidate this approach, but predictions based upon it agree well with the limited number of physiological experiments available.

† Also Department of Mathematics.

1. Introduction

The function of the lungs is the exchange of respiratory gases (oxygen and carbon dioxide) between the atmosphere and the circulating blood. This is accomplished by transporting air to and from the terminal respiratory units, the alveoli, by a complex system of branching tubes, the bronchial tree. Each alveolus is a thin-walled sac approximately 500 μm in diameter and surrounded by blood in thin-walled capillaries. It is here that transfer of gases between blood and air takes place.

In order that gas exchange should take place over as large an area as possible, the total cross-section of the bronchial tree increases rapidly with distance from the trachea (or windpipe) towards the alveoli. At each bifurcation the total cross-sectional area increases, although the daughter tubes individually are always smaller than the parent. Thus, in the human lung, while the trachea has a diameter of approximately 1·8 cm, the terminal airways, alveolar ducts after about 20 generations of branches, have diameters of approximately 0·041 cm, but their total cross-sectional area is about 12000 cm^2 (these figures are taken from the anatomical data of Weibel (1963)). Consequent upon the increase in area is a decrease in fluid velocity, and *a fortiori* of the Reynolds number, as the air passes down the lung. If, for example, the Reynolds number in the trachea is 8000† (corresponding to a volume flow rate of approximately 1600 cm^3/sec, which is well within the physiological range), that in the terminal airways will be approximately 0·04. It is clear that a fundamental prerequisite of any discussion of lung mechanics, from the point of view of studying either gas dispersion or the energetics of breathing, is a knowledge of the fluid mechanics of flow in branched tubes at all Reynolds numbers less than or of the order of 10000, and a technique for applying that knowledge to the lung itself.

In a recent series of papers (Schroter & Sudlow 1969; Pedley, Schroter & Sudlow 1970*a*, *b*) we have developed a method for tackling the problem. The resulting prediction of the pressure drop down the bronchial tree on inspiration, as a function of flow rate, agrees well with observation. We believe that the application of our approach is not restricted to physiology, and that it may be of some interest to fluid dynamicists in general. We present here a condensed version of this work, omitting most of the physiological details, and dwelling to a greater extent on the fluid mechanical implications.

The complexity of the problem compels us at the outset to make a number of simplifying assumptions. The airways are assumed to be straight circular tubes, with smooth walls, and the air is regarded as incompressible and of uniform density. In addition we restrict our discussion primarily to inspiratory flow (from the parent to the daughter tubes at each bifurcation: figure 1) and consider only steady flows. This last is probably the most controversial assumption from the physiological point of view, but it is argued that the unsteadiness has little effect on the fluid dynamics at the frequencies usually encountered during breathing (see Schroter & Sudlow 1969). A complete description of the

† Reynolds number in a pipe is here defined in terms of the diameter and mean velocity.

flow at every point of the airway network is evidently still out of the question, and we have found it convenient to regard the lung as made up of a large number of units, each consisting of a junction and the pair of daughter tubes issuing from it. The flow at any point in the daughter tubes will depend on many parameters, including the co-ordinates of the point, the Reynolds number in the tube, the ratios of the diameters of the daughter tubes to each other and to the parent tube, the angles which the axes of the daughter tubes make with that of the

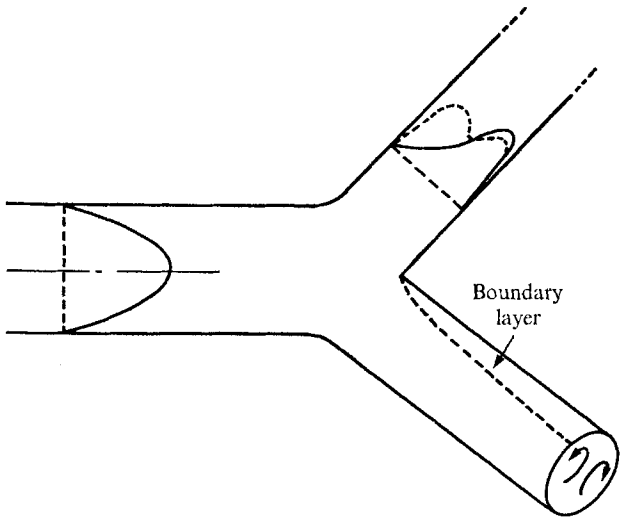

FIGURE 1. Qualitative picture of flow downstream of a single junction with Poiseuille flow in the parent tube. Direction of secondary motions and new boundary layer indicated in lower branch; velocity profiles in the plane of the junction (————) and in the normal plane (– – – – –) indicated in the upper branch.

parent, the shape of the junction (i.e. the radii of curvature of the walls at the junction), and the nature of the flow at the downstream end of the parent tube (which in general is a daughter of a previous junction, so the relative orientations of successive junctions is a further parameter to be considered when the units are joined). We have further restricted our discussion to symmetrical bifurcations, where the two daughter tubes are identical and make equal angles with the parent; the single 'branching angle' is then defined as the angle between the axes of the two daughter tubes.

A qualitative picture of the flow in a daughter tube can be built up for the case where an axisymmetric unidirectional laminar flow, with maximum velocity on the axis, is present in the parent tube. First of all the flow is split into two streams, so that a new boundary layer is formed on the inside wall of the daughter tubes, with maximum axial velocity just outside it. On top of that the flow turns a corner, so that the inertia of the faster moving fluid carries it towards the outside of the bend (the inside wall of the junction), which maintains the maximum axial velocity near that wall, and generates transverse velocity components, or secondary motions. Figure 1 contains qualitative pictures of the

expected axial velocity profiles in the plane of the junction and normal to it, together with a diagram of the secondary streamlines. In addition, depending on the sharpness of the corner in the outside wall of the junction, there may be a region of separated flow. All these effects will be modified downstream by the action of viscosity, but in a system like the lung, where the lengths of the tubes are at most four times their diameters, this modification will not be far advanced (for Reynolds numbers greater than approximately 100) before another junction is encountered, and the flow is disturbed again. No qualitative picture of the flow downstream of the second or subsequent junctions is readily available.

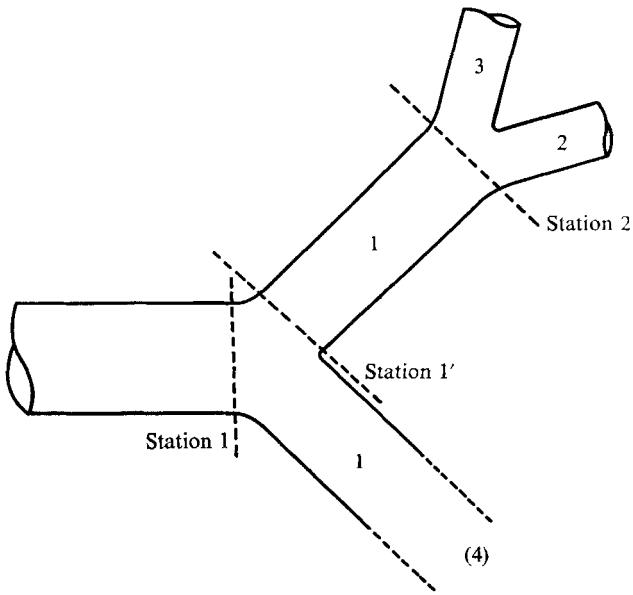

FIGURE 2. Diagram of model used, showing first- and second-generation branches. Case 1: first-generation branches. Cases 2 and 3: second-generation branches when both junctions are in the same plane. Case 4 (not shown): second-generation branches when second junction is normal to the first. Stations 1, 1′ and 2 define the limits of a junction and its daughter tube.

For this reason we set up an experiment in a model branched tube system containing two generations of junctions, with a geometry typical of the larger airways in the lung (see figure 2, noting the two different orientations of second-generation junctions). The branching angle and diameter ratio were the same at each junction. This experiment, described in some detail in §2, consisted of two parts. First, flow visualization studies confirmed the above qualitative picture of flow downstream of the first junction. Secondly, hot-wire velocity measurements were made, at various distances downstream of all junctions at several Reynolds numbers, from which axial velocity profiles were inferred. These profiles again confirm the above picture for a first junction, and reinforce the expectation that the flow downstream of a second junction is complex.

The question arises as to how these measured profiles can be used to make quantitative predictions in other systems and at other Reynolds numbers. In

particular, we would like to predict the pressure drop down a system of branched tubes as a function of flow rate. It was not possible in our experiments to measure the mean pressure drop directly, because the variations in pressure across a cross-section were as large as the overall downstream pressure drops. It is only in a system with many junctions or great lengths of tube that a mean pressure drop can be satisfactorily determined.

Let us consider the energy balance for a single 'unit', from station 1 at the downstream end of the parent tube to station 2 at the downstream end of the daughter tubes (figure 2). The rate at which the pressure forces do work on the fluid in the unit, plus the rate of loss of kinetic energy of that fluid (occasioned by the increase in cross-sectional area), is equal to the rate of dissipation of energy by viscosity. Let p, q and u represent the pressure, the total velocity, and the axial velocity at a point. If we now define the mean drop in pressure, ΔP, in kinetic energy per unit volume, ΔP_k, and in 'viscous pressure', ΔP_v, between the two stations, by

$$\left.\begin{aligned} \Delta P &= \left[\iint p u dA / \iint u dA\right]_2^1, \\ \Delta P_k &= \left[\iint \tfrac{1}{2}\rho q^2 u dA / \iint u dA\right]_2^1, \\ \Delta P_v &= D / \iint u dA, \end{aligned}\right\} \tag{1.1}$$

where the integrals are taken over the whole cross-section of the tubes at the relevant station, where D is the total viscous dissipation of energy in the unit, and where the denominator in each case is the volume flow rate, then the energy balance may be written

$$\Delta P + \Delta P_k = \Delta P_v. \tag{1.2}$$

A knowledge of the velocity field everywhere is sufficient for calculations of ΔP_v and ΔP_k and hence also for ΔP.

In §3 we explain how the limited velocity profiles obtained from our experiments can be used to estimate the energy dissipation in every case. This estimate is based on several approximations, of which the most important is that the volume of the region occupied by the junction itself (between stations 1 and 1′ in figure 2) is negligible compared with that of the daughter tubes (between stations 1′ and 2). Thus the dissipation D of (1.1) is taken to be equal to the dissipation in the daughter tubes only. It is implicit in this approximation that the viscous forces are not greater within the junction than beyond it, which is reasonable because the secondary motions are generated by inertial forces, and only subsequently modified by viscosity. The consequence of this approximation will be slightly to underestimate the total dissipation.

The results are presented in the form of two ratios Y and Z. Y is the ratio of the dissipation per unit length of a given tube at a distance x from the junction to the value this quantity would have if Poiseuille flow were present in that tube at that flow rate. Z is the ratio of the total dissipation in a given length of tube to the same quantity in Poiseuille flow. Since Poiseuille flow is associated with minimum viscous dissipation, both Y and Z must be greater than 1. Estimates of P_k are also given in §3.

In order to use these results predictively, it is necessary to have some understanding of the physical processes which govern the energy dissipation in a tube

downstream of a bifurcation. Our view of the mechanisms is foreshadowed by the above remark that when the fluid passes through a junction, a new boundary layer is formed on the inside wall of the daughter tubes, with maximum velocities outside it. This boundary layer will grow with distance downstream, as in classical entry flow, and the dissipation will be greatest within it, where the shear is high. Furthermore, the thickness of the boundary layer will not in general become comparable with the tube radius because another junction is encountered only three to four diameters downstream, and new boundary layers are again formed. We therefore postulate that the dependence of the dissipation on Reynolds number (Re) and on the number of diameters from the junction (x/d) is the same as in the simplest entry flow; this dependence is set out in §4. Since in our experiments the branching angles and diameter ratios of all junctions were the same, the only variable unaccounted for is the profile in the parent tube. (Although it is shown that both flat and parabolic profiles in the parent of the first junction lead to similar profiles in the daughters.) Thus in a given tube the ratios of the actual values of Y and Z to their entry flow values should be equal and constant ($= C$, say), but might vary from tube to tube. The results presented in §4 show that C is independent of both Re and x/d for each tube, and there is no significant difference between the values of C obtained from the three types of second-generation tube, although this common value is somewhat less than its value for first-generation tubes. The difference is still not large, and as a first attempt at predicting the pressure drop down a more complex system like the lung it has been ignored, and C set equal to the overall mean.

The above discussion, and our experiments, have been based on the assumption of laminar flow in all tubes. However, Reynolds numbers of the order of 10000 are encountered in the human trachea during rapid breathing, and hence turbulence will be present in the first few generations of airways. This point is taken up in §5 and the rather surprising conclusion is reached that the presence of turbulence at these Reynolds numbers has little effect on the overall dissipation (and hence pressure drop) in branched tubes, which will be underestimated by only a few per cent.

2. Experiments

The experiments were conducted in Y-shaped perspex models satisfying all the conditions described above and depicted in figure 2. The angle of branching at each junction was 70° and the diameter ratio of daughter to parent tube at each junction was 0·78 (the parent tube of the first junction had a diameter of 2·54 cm). The length of the tube between the first and second junction was 7·0 cm, with a length to diameter ratio of approximately 3·5. Most of the experiments were conducted in models with fairly sharp corners at the junctions, where the radius of curvature at the outer wall was equal to the radius of the parent tube. Some comparative studies were carried out with more rounded corners, where this radius of curvature was four times the radius of the parent tube, and although separation occurs in the former case but not the latter, the velocity profiles were not significantly altered except in regions of low shear

which contribute negligibly to the dissipation. The Reynolds number in the parent tube was varied between 280 and 1090, so that the Reynolds numbers in a tube of the second generation varied between 115 and 450.

The first junction was usually set at the end of a long straight pipe so that the flow entering the first junction was approximately Poiseuille flow (verified by hot-wire measurement of the profile), although in some cases it was set at the end of a very short pipe, when the profile was seen to be approximately flat, with thin boundary layers.

(*a*) *Flow visualization studies*

These were performed with a single junction only. Smoke was introduced with very low injection velocity through a series of small holes from a manifold fitted along the outside edge of one daughter tube. Secondary motions were observed at all Reynolds numbers studied, with either flat or parabolic profiles in the parent tube, figure 3(*a*) (plate 1) is an end view of the daughter tube, looking up towards the junction, and clearly shows the form of the secondary motions.

A few studies were made of expiratory flow (from the daughter tubes to the parent). Smoke was injected through a fine hypodermic some distance upstream of the junction. Figure 3(*b*) is an end view of the parent tube, showing the pattern of four secondary vortices, resulting from the simultaneous turning of two streams.

(*b*) *Velocity profile measurements*

These were made in the daughter tubes of both first- and second-generation junctions. A hot wire (12 μm diameter, 0·15 cm length) was introduced downstream and positioned by a micromanipulator. It was connected to a DISA constant temperature anemometer (Model 55A01), which was calibrated at frequent intervals during the experiments. Velocity profiles were measured at intervals of 1 or 2 cm downstream of each junction. Profiles in the plane of the junction and normal to it were obtained from point velocity measurements made at 0·1 cm steps across the diameters of the tube in those planes (except at 0·1 cm from the wall where accurate measurement was impossible). The long axis of the hot wire was always perpendicular to the axis of the tube being investigated, and lay in the plane of the junction. The readings were in all cases interpreted as measurements of axial velocity u, although the total heat transfer from the wire includes contributions from the transverse velocity components v and w. We assume that these contributions are negligible because (i) v and w are expected to be of smaller magnitude than u (from experimental and theoretical studies on flow in curved pipes by Ward-Smith (1963) and McConologue & Srivastava (1968) respectively); and (ii) the heat transfer from the wire depends primarily on the velocity normal to it (see Champagne, Sleicher & Wehrmann (1967) for the precise extent to which this is true), which here is essentially u.

An estimate of the systematic error associated with this interpretation was made from computations of the mean velocity through each tube, which is

known independently. The mean velocity calculated from the measured profiles (equation (3.7) below) was on average 7 % above the actual mean. To reduce the effect of these errors, all measured velocities were in each case reduced by ratio of the actual mean to the computed mean. After this adjustment, the errors in the measured velocities are certainly less than 10 %, except possibly

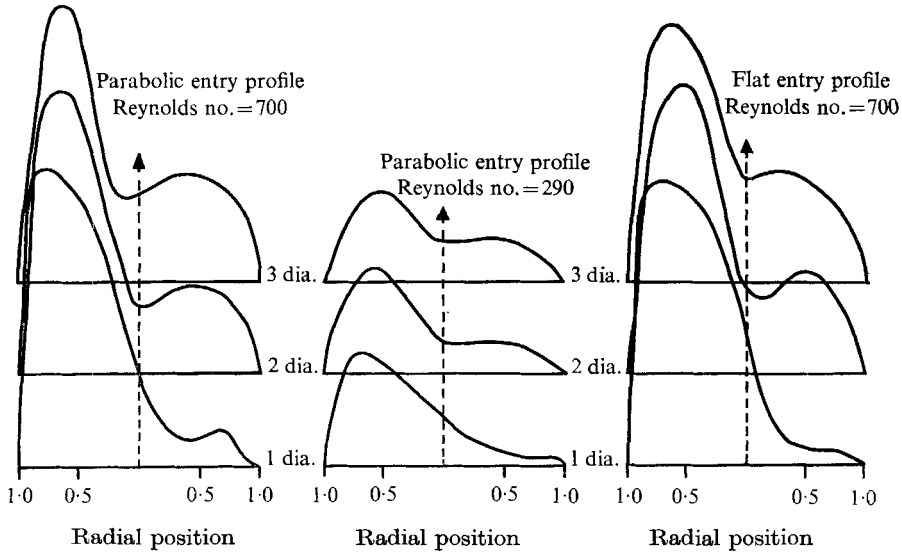

FIGURE 4. Changes in the velocity profile in the plane of the junction for case 1.

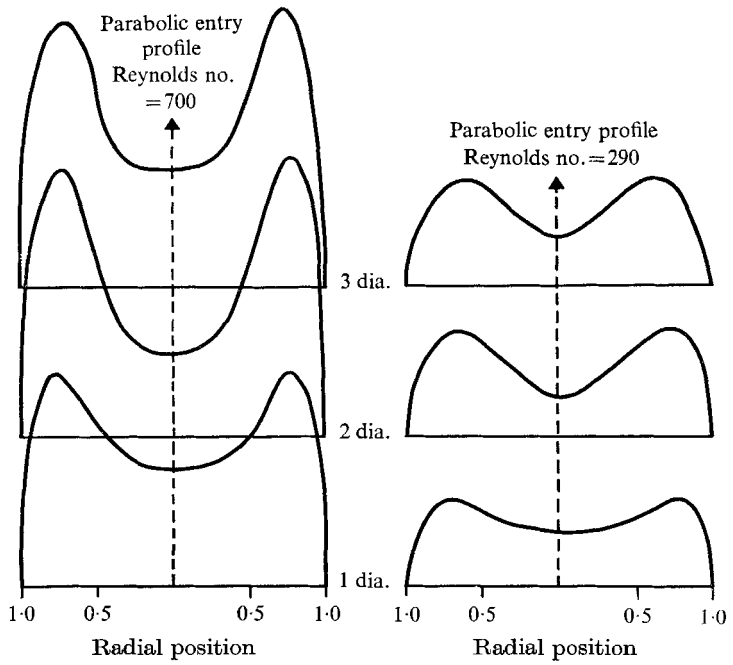

FIGURE 5. Changes in the velocity profile in the plane normal to the junction for case 1.

at the very lowest velocities which in any case contribute little to the integrals of (1.1).

Some typical profiles (not reduced in the above way) are shown in figures 4–6. Figure 4 shows profiles in the plane of the junction at three positions downstream of the first junction (case 1 in figure 2), at Reynolds numbers of 700 and 290

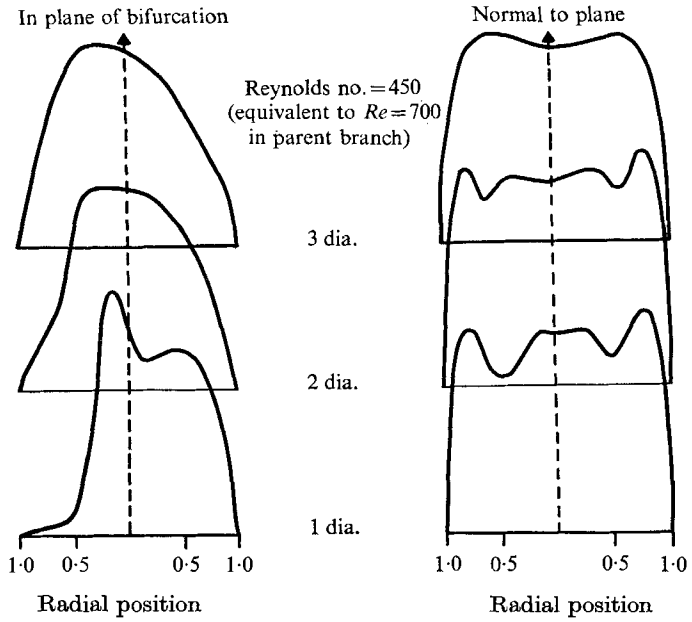

FIGURE 6. Changes in the velocity profile in the plane of the junction and normal to it for case 2.

with a parabolic entry profile, and at a Reynolds number of 700 with a flat entry profile, which can be seen to differ little from the parabolic case. Figure 5 shows profiles normal to the plane of the junction at Reynolds numbers of 700 and 290 with a parabolic entry profile. Note how the qualitative description of the flow given in the introduction is borne out by these profiles. Note too the slow development of the profiles downstream, recalling that when a second junction is added it will be placed only $3\frac{1}{2}$ diameters downstream of the first.

Figure 6 shows profiles in each plane at three positions downstream of a second junction, for a single Reynolds number of 450 (corresponding to a Reynolds number of 700 in the first generation tube). These profiles are for case 2 (figure 2), where the second junction is in the same plane as the first, and the flow is predominantly from the inside edge of the first-generation tube. Profiles were also obtained for cases 3 and 4 (see Schroter & Sudlow 1969). The profiles in the plane normal to the junction are approximately symmetrical in cases 1–3, as expected, but not in case 4 because the second junction is in a different plane from the first, and the secondary motions are therefore oriented differently. Incidentally, although the mean velocity in cases 2 and 3 might be expected to be different (for a given flow rate in the parent tube) because of the asymmetry of the entry profile, the computed means did not differ significantly. The rapid

adjustment of the profile in the plane of the junction in the case shown, to an almost symmetrical form, is probably a consequence of the fact that the secondary motions set up by the second junction in this case are in the opposite sense to those set up by the first junction.

3. Energy dissipation

It is convenient to describe the flow in a given tube in terms of cylindrical polar co-ordinates (x, r, θ), where the tube surface is the cylinder $r = a$, and the zero of x occurs at that station where the walls of the tube first become parallel (see figure 2). Let the components of velocity in the axial, radial, and tangential directions be u, v, w respectively. The dissipation per unit volume of the fluid ($\mathscr{D}$) at any point can then be written as the sum of squares of expressions containing u, v, w and their space derivatives. If we assume that v and w are small compared with u, by a factor of order of magnitude ϵ, say, and that x-derivatives are small compared with r- and θ-derivatives by a similar factor (justified by the profiles of figures 4–6, and by an appeal to the continuity equation, from which $\partial u/\partial x$ is seen to be of the same order as $\partial v/\partial r$, etc.), then the exact expression for $\mathscr{D}$ can be replaced by the approximate formula

$$\mathscr{D} = \mu\left\{\left(\frac{\partial u}{\partial r}\right)^2 + \frac{1}{r^2}\left(\frac{\partial u}{\partial \theta}\right)^2\right\}, \tag{3.1}$$

where neglected terms are of the second order in ϵ. This approximation will result in a slight underestimate of $\mathscr{D}$. The dissipation per unit length of the tube at a given value of x is then given by

$$D_1(x) = \int_0^{2\pi}\int_0^a \mathscr{D} r\, dr\, d\theta, \tag{3.2}$$

and the total dissipation in the length of tube between x_1 and x_2 is

$$D = \int_{x_1}^{x_2} D_1(x)\, dx. \tag{3.3}$$

Calculation of these quantities requires that we know u as a function of x, r and θ. In fact we have isolated velocity measurements at certain values of r in two perpendicular planes (i.e. at $\theta = 0, \frac{1}{2}\pi, \pi, \frac{3}{2}\pi$) for a few given values of x. Standard interpolative procedures are used to give smooth functions for $u(r)$ at these values of θ, and the simplest smooth periodic function of θ which has the correct form at the four given values of θ is

$$u(r,\theta) = g_1(r) + g_2(r)\cos 2\theta + g_3(r)\sin\theta + g_4(r)\cos\theta, \tag{3.4}$$

where

$$\left.\begin{aligned} g_1(r) &= \tfrac{1}{4}[u(r,0) + u(r,\tfrac{1}{2}\pi) + u(r,\pi) + u(r,\tfrac{3}{2}\pi)],\\ g_2(r) &= \tfrac{1}{4}[u(r,0) - u(r,\tfrac{1}{2}\pi) + u(r,\pi) - u(r,\tfrac{3}{2}\pi)],\\ g_3(r) &= \tfrac{1}{2}[u(r,\tfrac{1}{2}\pi) - u(r,\tfrac{3}{2}\pi)],\\ g_4(r) &= \tfrac{1}{2}[u(r,0) - u(r,\pi)]. \end{aligned}\right\} \tag{3.5}$$

Substitution of (3.4) into (3.1) and (3.2) then gives

$$D_1(x) = \pi\mu \int_0^a \left\{ \frac{1}{r^2}(4g_2^2 + g_3^2 + g_4^2) + (2g_1'^2 + g_2'^2 + g_3'^2 + g_4'^2) \right\} r\,dr, \tag{3.6}$$

where a prime denotes differentiation with respect to r.

	$\overline{U}$		$Y(x)$				
	(cm/sec)	Re	$x = 2$ cm	$x = 3$ cm	$x = 4$ cm	$x = 5$ cm	$x = 6$ cm
Case	52·4	699	4·69	—	3·62	—	2·73
1	41·6	555	5·09	—	2·96	—	2·38
	31·3	417	4·10	—	2·98	—	2·06
	22·0	293	2·82	—	2·16	—	1·65
	13·3	177	3·24	—	1·68	—	1·47
Case	40·9	436	2·57	2·22	1·80	1·76	1·41
2	32·5	347	1·64	1·82	1·36	1·34	1·38
	17·2	183	1·25	1·17	1·17	1·21	1·17
Case	40·9	436	2·48	2·62	1·97	2·34	1·56
3	32·5	347	2·23	2·66	1·67	2·19	1·32
	17·2	183	1·61	1·39	1·25	1·33	1·12
Case	40·9	436	2·34	2·09	2·21	1·79	1·53
4	32·5	347	2·05	1·80	1·75	1·49	1·29
	17·2	183	1·50	1·41	1·53	1·21	1·16

TABLE 1

In each tube, at each Reynolds number, and at each value of x for which profiles were available ($x = 2$, 4, 6 cm in case 1, and $x = 2$, 3, 4, 5, 6 cm in cases 2, 3, 4), the integral in (3.6) was evaluated numerically. In each case we have computed the ratio

$$Y(x) = D_1(x)/D_{1P},$$

where

$$D_{1P} = 8\pi\mu\overline{U}^2$$

is the value of $D_1(x)$ in Poiseuille flow, and $\overline{U}$ is the mean velocity in the tube considered. (As explained above, the value of $\overline{U}$ calculated from the measured profiles and the equation

$$\overline{U} = \frac{1}{\pi a^2}\int_0^{2\pi}\int_0^a u(r,\theta)\,r\,dr\,d\theta = \frac{2}{a^2}\int_0^a g_1(r)\,dr, \tag{3.7}$$

did not exactly coincide with the value obtained from the known volume flow rate. In general the computed value was higher, the average excess being 7 %, with a standard deviation of less than 9 %. The latter figure is a measure of the errors involved in the hot-wire readings and the interpolative procedures outlined above.) The calculated values of $Y(x)$, $\overline{U}$ and the Reynolds number $Re = 2\overline{U}a\rho/\mu$ are given in table 1. Notice that Y increases with Re and decreases with x, as is to be expected since larger Re and smaller x correspond to flows further removed from Poiseuille flow. The total dissipation D in each tube between $x = x_1 = 2$ cm and $x = x_2 = 6$ cm was then computed from (3.3) using Simpson's rule. This is again compared with its value in Poiseuille flow [$D_P = 8\pi\mu\overline{U}^2(x_2 - x_1)$] by means

of the ratio $Z = D/D_P$. These results are presented in table 2. Z increases with Re.

Methods similar to the above were also used to compute the kinetic energy per unit volume P_k (equation (1.1)). Neglecting transverse velocities again, the formula for P_k is

$$P_k = \frac{1}{\pi a^2 \overline{U}} \int_0^{2\pi} \int_0^a \tfrac{1}{2}\rho u^3 r \, dr \, d\theta. \tag{3.8}$$

	Re	699	555	417	293	177
Case 1	Z	3·65	3·22	3·01	2·18	1·91
	Re	436	347	183		
Case 2	Z	1·96	1·53	1·19		
Case 3	Z	2·32	2·19	1·34		
Case 4	Z	1·98	1·67	1·35		

TABLE 2

This quantity was calculated in each case, for each value of x. However, it is only at the downstream end of each pipe (stations 1 or 2 of figure 1) that we require to know P_k. Surprisingly, if at $x = 6$ cm we write

$$P_k = B\rho\overline{U}^2, \tag{3.9}$$

the quantity B, which has the value 1 for a parabolic profile and $\frac{1}{2}$ for a flat profile, has no systematic dependence on Re or on the type of tube. Its mean value was 0·85, which we assume to be universal for branched tubes of this branching angle and diameter ratio.

4. Entry flow model

The ratios Y and Z in tables 1 and 2 vary with Reynolds number and Y varies with x. As explained in the introduction, we make the hypothesis that these variations are the same as in a simple entry flow, and then use the results in tables 1 and 2 to verify it.

The simplest entry flow in a tube occurs when the entry profile is flat and of magnitude $\overline{U}$. We assume that within the boundary layer the velocity profile is linear, and outside the boundary layer it is flat and of magnitude U_0 (see figure 7). This is a very simple version of the Pohlhausen method described by Goldstein (1938, §139). The boundary-layer thickness ($a\delta$) increases with x and, as long as $\delta \ll 1$, we may assume that it grows in the same way as the boundary layer on a flat plate:

$$a\delta = (2\mu x/\rho U_0)^{\frac{1}{2}}. \tag{4.1}$$

The dissipation in this flow (occurring solely in the boundary layer) and the magnitude of U_0 can easily be calculated from equations (3.1), (3.2), (3.3) and (3.7). The ratios Y and Z associated with this flow can be expanded in powers

of δ, and the leading terms, when expressed in terms of the dimensionless quantities Re and x/d (where $d = 2a$), are

$$Y(x) \approx \frac{1}{8\sqrt{2}} \left(Re \frac{d}{x}\right)^{\frac{1}{2}}, \tag{4.2}$$

$$Z \approx \frac{Re^{\frac{1}{2}}}{4\sqrt{2}\{(x_2/d)^{\frac{1}{2}} + (x_1/d)^{\frac{1}{2}}\}}. \tag{4.3}$$

Now, we clearly do not expect exact numerical agreement between the experimental values of Y and Z and these equations, but we do expect the same dependence on Re and x/d in each tube, as long as $\delta \ll 1$ everywhere. (This

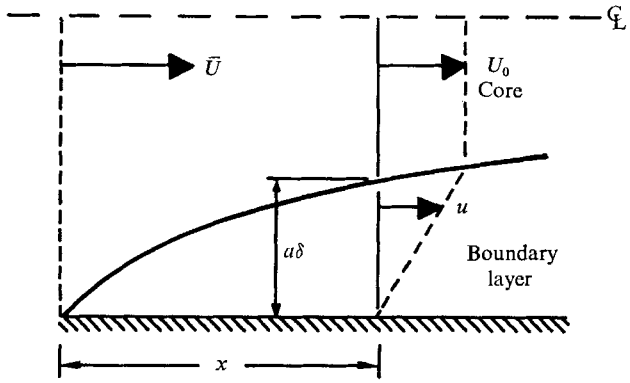

FIGURE 7. Scheme for calculation of dissipation in an entry flow.

condition requires that $L/d \ll Re/8$, where L is the length of the tube. In all our experiments $L/d = 3{\cdot}5$ and the minimum value of Re was 177, so the maximum value of δ was about 0·38. In the majority of cases δ was much less than 0·38, so our simple model is applicable.) The ratio of the values of $Y(x)$ from table 1 with the value given by (4.2) should be a constant, C, independent of Re and x/d, but possibly varying from tube to tube. The ratio of the values of Z from table 2 with the value given by (4.3) should also be equal to C. The values of C thus computed from Y and Z are presented in tables 3 and 4 respectively.

From these tables we can see that (i) there is no systematic variation of C with Re; (ii) there is no systematic variation of C with x/d, except in case 1 where there is a slight decrease; (iii) there is no significant difference between the values of C computed from cases 2–4; (iv) there is a noticeable difference between the values of C for case 1 (single junction) on the one hand, and cases 2–4 on the other.

Clearly the proposed model gives the correct dependence of Y and Z on Re and x/d, and we may presume that the same value of the constant C may be used for all tubes of a given generation. However, the value of C does appear to depend on generation number. In our application of this work to the lung, we have ignored this dependence, and used the average of all the values in table 4: $C = 1{\cdot}85$. (The average from table 3 is $C = 1{\cdot}77$.) The difference between the

means for generations 1 and 2 and the overall mean was only of the same order as the estimated experimental and interpolative error: less than 20%.

Our final result is that the ratio of the total dissipation in a tube downstream of a bifurcation (with the given branching angle and diameter ratio) to its value in Poiseuille flow is given by C times the value of Z obtained from (4.3) with $x_1 = 0$ and $x_2 = L$. That is

$$Z = \frac{C}{4\sqrt{2}}\left(Re\frac{d}{L}\right)^{\frac{1}{2}}, \tag{4.4}$$

		C				
	Re	$x = 2$	$x = 3$	$x = 4$	$x = 5$	$x = 6$
Case 1	699	2·01	—	2·19	—	2·03
	555	2·44	—	2·01	—	1·98
	417	2·27	—	2·33	—	1·97
	293	1·86	—	2·02	—	1·88
	177	2·75	—	2·02	—	2·16
Case 2	436	1·56	1·65	1·54	1·68	1·48
	347	1·11	1·52	1·31	1·44	1·63
	183	1·17	1·33	1·55	1·78	1·89
Case 3	436	1·50	1·94	1·69	2·24	1·64
	347	1·51	2·21	1·60	2·35	1·55
	183	1·51	1·58	1·65	1·97	1·81
Case 4	436	1·42	1·55	1·89	1·71	1·61
	347	1·40	1·50	1·68	1·60	1·52
	183	1·40	1·61	2·02	1·79	1·88

TABLE 3

	Re	699	555	417	293	177
Case 1	C	2·13	2·11	2·28	1·97	2·21

	Re	436	347	183
Case 2	C	1·62	1·42	1·52
Case 3	C	1·92	2·03	1·71
Case 4	C	1·64	1·55	1·72

TABLE 4

where $C = 1{\cdot}85$. Note that for Reynolds numbers less than 32·7 (if $L/d = 3{\cdot}5$) Z turns out to be less than one. This is clearly impossible, and indicates that the model breaks down for such low Reynolds numbers. In these circumstances, Z should be set equal to one, the best estimate available.

Z is also the ratio of viscous pressure drop in a tube (ΔP_v, see (1.1)) to the Poiseuille pressure drop. Thus in a complex system in which (4.4) is applicable at every junction, the overall viscous pressure drop is related to the volume flow rate Q and the fluid density ρ and viscosity μ by

$$\Delta P_v = K(\mu\rho)^{\frac{1}{2}}Q^{\frac{3}{2}}, \tag{4.5}$$

where K depends only on the geometry and dimensions of the system.

5. Effect of turbulence

When the Reynolds number in the trachea exceeds about 2000, the flow will be turbulent. When it is as high as 10000, this turbulence will persist into the fourth and the fifth generation of airways (Owen 1969). Since both theory (Pedley, Schroter & Sudlow 1970*b*) and experiment (Macklem, Fraser & Bates 1963) indicate that the majority of the pressure drop occurs in the first few generations, it is necessary to consider the effect of the turbulence on the pressure drop, and in particular to ascertain how it will alter (4.4). We should point out that the ideas set out below have not yet been tested experimentally, and can only be regarded as indications of what happens.

In a turbulent flow, two separate contributions to the dissipation can be distinguished: (*a*) the dissipation associated with the mean velocity field (in general different from its laminar value), and (*b*) the dissipation of the turbulent eddies. Let us consider (*a*) first.

(*a*) The laminar model of §4 was based on the assumption that the dissipation in the flow downstream of a junction occurs primarily in the thin boundary layers which start on the inside edge of the junction. In turbulent flow, new boundary layers will be formed at the bifurcation in the same way, and will initially be laminar.

If they remain laminar, with only the core turbulent, the dissipation will, at least dimensionally, be the same as in completely laminar flow. If the boundary layers become turbulent, they will be thicker, and their contribution to the dissipation of the mean flow will decrease (but the eddy dissipation will be greatly increased). For a laminar boundary layer on a flat plate at zero pressure gradient, the critical Reynolds number, Re_{δ_1}, for transition to turbulence, based on the displacement thickness

$$\delta_1 = 1{\cdot}73(\nu x/U_0)^{\frac{1}{2}},$$

is approximately 3400 (this is not to be confused with the theoretically calculated critical Reynolds number of about 420, above which infinitesimal disturbances grow with time). There are three reasons why the critical value of Re_{δ_1}, should be very much less in our case.

First, there is turbulence in the core of the tube outside the boundary layer, which will trigger off boundary-layer transition at a much smaller Reynolds number. Dryden (1936) gives the value of about 530 when the intensity of turbulence in the free stream is 3 %, which is approximately the intensity in the core in fully-developed turbulent pipe flow (Hall 1938), and is the highest intensity whose effect on boundary-layer transition has been recorded.

The second possible mechanism of boundary-layer transition is that of Taylor–Görtler vortices, associated with flow over a concave surface. According to Schlichting (1960, p. 443) transition will occur if

$$Re_\theta(\theta/R)^{\frac{1}{2}} \gtrsim 7,$$

where θ is the momentum thickness of the boundary layer ($\approx 0{\cdot}38\delta_1$), Re_θ is the Reynolds number based upon it, and R is the radius of curvature of the

concave surface. Note that the value of 7 is again about 20 times the critical value for the growth of infinitesimal disturbances. Let us assume that the transverse velocity components in a daughter tube are approximately 10% of the longitudinal component. R, then is the radius of curvature, at the extremity of its minor axis, of the ellipse which is formed by the intersection of the cylindrical tube with a plane making an angle $\tan^{-1}(0{\cdot}1)$ with its generators: $R \approx 50d$. From this we can calculate that the critical value of Re_{δ_1} for transition due to Taylor–Görtler vortices is approximately $33\,Re^{\frac{1}{2}}$.

The final mechanism of boundary-layer transition in our case is associated with the secondary motions, like that investigated by Gregory, Stuart & Walker (1955). They realized that the transverse pressure gradients required for secondary motions will mean that, in directions which are not parallel to the flow just outside the boundary layer, the velocity profile within the boundary layer has a point of inflexion. These motions will therefore be strongly unstable, and the transition value of Re_{δ_1} in the case they considered (the boundary layer over a rotating disk) was reduced to about 680. However, in another example, of this type of instability (flow over a swept-back wing) Owen & Randell (1953) found a transition value of Re_{δ_1} of about 400. Let us assume that this value is appropriate in our case. It seems likely that the strength of the two latter instabilities will preclude their being greatly affected by turbulence in the core.

Thus the boundary layer is expected to remain laminar as long as

$$Re < \min\left\{\frac{53\,000}{(x/d)}, \left(\frac{360}{x/d}\right)^3\right\}.$$

In the lung and in our models, $x/d \leqslant 3{\cdot}5$, so the second quantity in the bracket is everywhere greater than 10^6, and the first quantity gives the lower critical value of Re, indicating that the third mechanism of transition is dominant in this case. For the boundary layer to remain laminar for all $x/d < 3{\cdot}5$, Re must be less than about 15000 (this number would be reduced to about 4000 if the critical value of Re_{δ_1} for the third mechanism of transition were 200 not 400). Thus, we do expect the boundary layer to remain laminar when the Reynolds number in the daughter tube is less than 15000; the model outlined in §4 is applicable even when the core is turbulent, and the dissipation associated with the mean velocity profile is given by (4.4) with some value of C.

The value taken by C depends on the details of the mean velocity profile, of which, in turbulent flow, we have no direct observations. However, the secondary motions, and the distortions of the axial velocity profile, are generated in a purely inertial manner, and there is no obvious way in which the turbulence would affect them, apart from a more rapid smoothing out of velocity gradients in the core of the tube. Furthermore, the velocity profile entering from the trachea is likely to have the same general shape as in laminar flow, with a peak on the axis, since it consists of a turbulent jet emanating from the constriction at the larynx, and interacting with the walls somewhat before the first bifurcation (Owen 1969). In the absence of experiments on turbulent flow in branched tubes, it seems reasonable to use the laminar value of 1·85 for C.

(*b*) We must now consider the dissipation associated with the turbulent eddies. We shall assess its importance on the untested but plausible assumption

that it is of the same order of magnitude as in fully-developed turbulent pipe flow at the same Reynolds number. This assumption is probably an over-simplification, as it ignores the fact that there are regions both of unusually high and of unusually low shear in the daughter tubes, which will also be regions of high and low turbulent intensity (and hence dissipation) respectively. But as long as the boundary layer itself remains laminar, the dissipation is unlikely to be enormously enhanced. In any case, we shall see that even if the eddy dissipation is increased five times over its value in fully-developed flow, it will contribute less than 30% of the total dissipation at the maximum Reynolds number of 10^4. The eddy dissipation in fully-developed pipe flow can be evaluated by subtracting the dissipation associated with the known mean profile from the total dissipation in that flow, inferred from experimentally determined skin friction coefficients. Let us take the mean velocity profile to be linear very near the wall and logarithmic elsewhere (although this is strictly valid only for $Re > 10^4$; Patel & Head (1969)), as follows:

$$\left.\begin{aligned} u(y)/u_\tau &= u_\tau y/\nu \quad (0 < y < a_0), \\ &= \frac{1}{K}\left[\log_e \frac{u_\tau y}{\nu} + A\right] \quad (a_0 < y < a), \end{aligned}\right\} \tag{5.1}$$

where u_τ is the friction velocity, y the distance from the pipe wall, K, A are constants equal to 0·41, 2·4 respectively (Townsend 1956, p. 202), and a_0 is chosen so that $u(y)$ is a continuous function. We calculate the dissipation associated with this profile from (3.1) and (3.2), and the mean velocity in the pipe from (3.7). We can then express both the Reynolds number in the pipe (Re) and the ratio of the calculated dissipation to that in Poiseuille flow (Z') in terms of the friction Reynolds number $Re_\tau = u_\tau a/\nu$:

$$Re = \frac{2}{K} Re_\tau \log_e Re_\tau + \frac{2A-3}{K} Re_\tau + \frac{4\alpha}{K} - 4\alpha^2 + \left(2\alpha^3 - \frac{\alpha^2}{K}\right)\frac{1}{Re_\tau}, \tag{5.2}$$

$$Z' = \frac{Re_\tau^2}{Re^2}\left\{\left(\alpha + \frac{1}{\alpha K^2}\right) Re_\tau - \frac{1}{K^2}\log_e Re_\tau + \frac{\alpha}{K} - \frac{A+1}{K} - \alpha^2\right\}, \tag{5.3}$$

where $\alpha = u_\tau a_0/\nu = 12$ (this and all subsequent results are given to two significant figures).

The ratio of total dissipation in fully-developed turbulent pipe flow to that in Poiseuille flow at the same Reynolds number (Z_T) is given by the ratio of the skin friction coefficients C_f: for turbulent flow, $C_f = 0{\cdot}079 Re^{-\frac{1}{4}}$ (valid for $Re > 3000$; Patel & Head 1969), and for Poiseuille flow, $C_f = 16/Re$. Thus

$$Z_T = 0{\cdot}0049 Re^{\frac{3}{4}}. \tag{5.4}$$

As examples, let us take two Reynolds numbers in the range of interest:

(i) $Re = 5000$. From (5.2), $Re_\tau = 180$, whence from (5.3), $Z' = 2{\cdot}9$. But from (5.4) $Z_T = 2{\cdot}9$ also. Thus the dissipation in the eddies (proportional to $Z_T - Z'$) contributes a very small amount to the total: less than 4%. Furthermore, the value of Z at this Reynolds number, in a branched tube for which $L/d = 3{\cdot}5$, is equal to 12, from (4.4). Thus, if the dissipation of the eddies is of the same order of magnitude as in fully-developed flow, it contributes less than 1% of the total.

(ii) $Re = 10000$. From (5.2), $Re_\tau = 320$, whence from (5.3), $Z' = 3{\cdot}9$. But from

(5.4) $Z_T = 4{\cdot}9$. Thus the eddies contribute about 20 % to the total dissipation in fully-developed pipe flow. However, at this Reynolds number, the value of Z from (4.4) is approximately 17, so the eddies contribute less than 6 % of the total dissipation in branched tubes.

These results are not significantly changed if we assume that the mean velocity in fully-developed pipe flow obeys a 1/7 power law rather than a logarithmic law.

For $Re \leqslant 10\,000$, therefore, we are justified in neglecting the contribution of turbulent eddies and in using (4.4) for Z. As the Reynolds number increases above this value the boundary layers become turbulent, and the eddies contribute a greater proportion of the total dissipation, so that (4.4) leads to an increasingly severe underestimate of the dissipation, and our model is inadequate.

6. Discussion

The results of applying (4.4) to every junction in a symmetric model of the lung (using (3.9) for the kinetic energy term in (1.2)) are exhaustively set out in Pedley *et al.* (1970*b*). It may be remarked here that their agreement with physiological experiments is considerably closer than that of previous theories, based on Poiseuille flow in every tube (Green 1965; Horsfield & Cumming 1968). Because most of the systematic errors involved in our model (see above) lead to underestimates of the dissipation, we would expect the predicted pressure drops still to be too low. However, the as yet limited number of controlled experiments, and the inherent variability of physiological parameters, make these differences difficult to observe.

Although the agreement of our predictions with physiological experiments is heartening, we should not regard the work described above as more than the beginning of a complete study of flow in branched tubes. The chief requirement is a much fuller series of model experiments. For a given branching angle and diameter ratio, detailed information on the complete velocity field (v and w as well as u) should be obtained at many more points within a tube, so that any interpolation method can be used with confidence to give u, v, w as functions of x, r, θ and hence to compute the dissipation accurately. This must be repeated for a wide range of Reynolds numbers, including those for which the flow is turbulent in one or more generations, in order to provide a complete test both of equation (4.4) and the ideas of §5. Then again, the influence of generation number on the value of C should be investigated by building models with a greater number of generations. Finally, the branching angle and diameter ratio should be varied independently, and the experiments repeated at every new value. Comparative experiments should also be done to discover the effect of varying the curvature of the side walls and flow dividers at junctions.†

In conclusion, mention should be made of a separate series of experiments which we are currently performing to test our results in the absence of the complicating features present in physiological experiments. A six-generation network of branched glass tubes has been constructed so that every junction

† Such a series of experiments is currently being carried out in the Physiological Flow Studies Unit, Imperial College by Mr D. E. Olson.

has a branching angle of approximately 70° and a diameter ratio of approximately 0·78. The parent tube has a diameter of 2·4 cm. At a wide range of 'inspiratory' flow-rates the pressure drop down the system is measured. So, too, are the velocity profiles in the parent tube and the final daughter tubes, so that the change in kinetic energy per unit volume may be computed. The viscous pressure drop can be inferred from these measurements. Preliminary results show excellent agreement with the theoretical estimate of the viscous pressure drop obtained by applying (4.4) to every tube in the system, for parent tube Reynolds numbers between 10^3 and 10^4. Thus it seems that our general approach is a valid one, and, in particular, that our otherwise unverified ideas on the effect of turbulence are basically correct.

We are grateful to the Royal Society, the Asthma Research Council, and the Tobacco Research Council for their financial support.

REFERENCES

CHAMPAGNE, F. H., SLEICHER, C. A. & WEHRMANN, O. H. 1967 Turbulence measurements with inclined hot-wires. Part 1. Heat transfer experiments with inclined hot-wire. *J. Fluid Mech.* **28**, 153.

DRYDEN, H. L. 1936 Air flow in the boundary layer near a plate. *NACA Rep.* no. 562.

GOLDSTEIN, S. 1938 *Modern Developments in Fluid Mechanics.* Oxford: Clarendon Press.

GREEN, M. 1965 How big are the bronchioles? *St Thomas's Hospital Gazette*, **63**, 136.

GREGORY, N., STUART, J. T. & WALKER, W. S. 1955 On the stability of three-dimensional boundary layers with application to the flow due to a rotating disk. *Phil. Trans. Roy. Soc.* A **248**, 155.

HALL, A. A. 1938 Measurements of the intensity and scale of turbulence. *Aero. Res. Comm. R & M* no. 1842.

HORSFIELD, K. & CUMMING, G. 1968 Functional consequences of airway morphology. *J. appl. Physiol.* **24**, 384.

MCCONALOGUE, D. J. & SRIVASTAVA, R. S. 1968 Motion of a fluid in a curved tube. *Proc. Roy. Soc.* A **307**, 37.

MACKLEM, P. T., FRASER, R. G. & BATES, D. V. 1963 Bronchial pressures and dimension in health and in obstructive airways disease. *J. appl. Physiol.* **18**, 699.

OWEN, P. R. 1969 Turbulent flow and particle deposition in the trachea. In *CIBA Symposium on Circulatory and Respiratory Mass Transport.* London: J. and A. Churchill.

OWEN, P. R. & RANDALL, D. G. 1953 Boundary layer transition on a swept-back wing—a further investigation. *R.A.E. Tech. Rep. Memo.* no. Aero. 330.

PATEL, V. C. & HEAD, M. R. 1969 Some observations on skin friction and velocity profiles in fully developed pipe and channel flows. *J. Fluid Mech.* **38**, 181.

PEDLEY, T. J., SCHROTER, R. C. & SUDLOW, M. F. 1970*a* Energy losses and pressure drop in models of human airways. *Respir. Physiol.* **9**, 371.

PEDLEY, T. J., SCHROTER, R. C. & SUDLOW, M. F. 1970*b* The prediction of pressure drop and variation of resistance within the human bronchial airways. *Respir. Physiol.* **9**, 387.

SCHLICHTING, H. 1960 *Boundary Layer Theory*, New York: McGraw-Hill.

SCHROTER, R. C. & SUDLOW, M. F. 1969 Flow patterns in models of human bronchial airways. *Respir. Physiol.* **7**, 341.

TOWNSEND, A. A. 1956 *The Structure of Turbulent Shear Flow.* Cambridge University Press.

WARD-SMITH, A. J. 1963 Flow and pressure losses in smooth pipe bends of constant cross-section. *J. Roy. Aero. Soc.* **67**, 437.

WEIBEL, E. R. 1963 *Morphometry of the Human Lung.* Berlin: Springer.

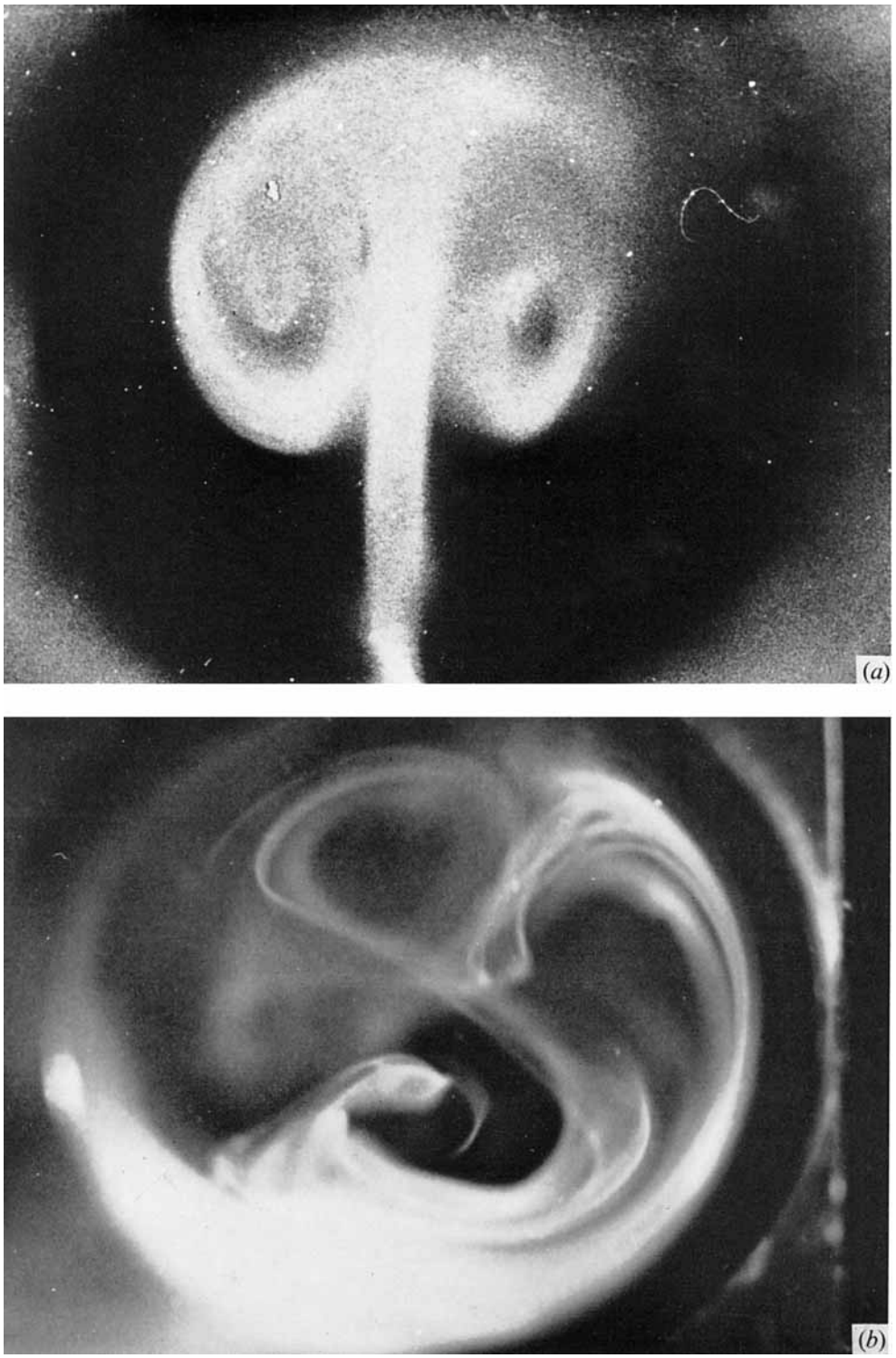

FIGURE 3. (*a*) End view of a daughter branch of a single junction showing secondary motions when flow is from the parent to the daughters. (*b*) End view of parent tube of a single junction showing secondary motions when flow is from the daughters to the parent.